Journal of Structural Geology, Vol. 10, No. 8, pp. 895 to 904, 1988
Printed in Great Britain

0191-8141/88 $03.00 + 0.00

Experimental shear zones and magnetic fabrics

G. J. BORRADAILE and C. ALFORD

Geology Department, Lakehead University, Thunder Bay, Ontario, Canada P7B 5E1

(*Received* 26 *November* 1987; *accepted in revised form* 7 *July* 1988)

Abstract—Magnetic fabric analysis has been used as a non-destructive means of detecting petrofabric development during experimentally produced multi-stage, transpressive deformations in 'shear zones'. Artificial, magnetite-bearing silicate sands and calcite sands, bonded with Portland cement, were deformed at room temperature and at 100 and 150 MPa confining pressure. The slip-rate for the shear zone walls was 0.73×10^{-4} mm s^{-1} and the maximum shear strains were about 0.38, across zones that were initially about 5 mm thick. The magnetic fabric ellipsoid rapidly spins so that the maximum and intermediate susceptibilities tend to become parallel to the shear zone walls throughout the sheared zone. The ellipsoid becomes increasingly oblate with progressive deformation. However, in all cases, the anisotropy is strongly influenced by the pre-deformation magnetic fabric. During deformation the cement gel collapses so that cataclasis of the mineral grains is suppressed. In the quartz–feldspar aggregates the magnetite's alignment is accommodated by particulate flow (intergranular displacements) of the grains. In the calcite aggregates stronger magnetic fabrics develop due to plastic deformation of calcite grains as well as particulate flow. However, the calcite grain fabrics are somewhat linear ($L \geq S$) whereas the magnetic fabrics are planar ($S > L$). The preferred dimensional orientations of magnetite are weak and it is possible that the magnetic fabrics are due to intragranular rearrangements of magnetic domains.

The transpressive shear zones are much more efficient than axial-symmetric shortening in the increase of anisotropy of the magnetic fabrics, especially in the case of the calcite aggregates. This suggests that flow laws derived for axial-symmetric shortening experiments may not be appropriate for non-coaxial strain histories such as those of shear zones.

INTRODUCTION

THE anisotropy of magnetic susceptibility can be represented by an ellipsoid that we shall term the magnetic fabric ellipsoid. It has been shown elsewhere that its principal directions can be a useful indication of the orientations of principal strains in both naturally and experimentally deformed rocks (Hrouda 1982, Borradaile & Alford 1987). Such relationships are not universally valid (e.g. Borradaile & Tarling 1981), but the magnetic fabric method is a useful way of rapidly remote-sensing the principal fabric directions of the dominant ferrimagnetic or paramagnetic minerals in deformed rocks. With further careful evaluation it may be possible to infer that these directions are also close in orientation to principal strain directions.

Magnetite is important as a ferrimagnetic accessory mineral because the magnetic anisotropy of individual grains is controlled by their shapes. The maximum susceptibility is nearly parallel to the longest dimension of a grain and the minimum value is close to the shortest dimension. Even slightly non-equidimensional grains give precisely measurable magnetic anisotropies, thus, a weak preferred orientation of grains gives a strong anisotropy of the bulk susceptibility of a polygranular sample. In the present study the magnetic fabrics are believed to result from the rotation of essentially rigid magnetite grains, because there is no microscopic evidence of ductile deformation of the grains. It is possible, however, that internal stress-induced rearrangements within the magnetite grains could influence the anisotropy.

Magnitudes of strain cannot be ascertained from magnetic measurements with much confidence. Nevertheless, weak correlations between magnitudes of susceptibility and principal strain values may exist, notwithstanding the fact that one method used to determine such correlations has been shown to be erroneous (Borradaile & Mothersill 1984). Although it is of less practical use, *changes* in susceptibility anisotropy have been found to correlate with strain quite strongly in certain pure shear experiments, with specific initial orientations of the magnetic fabric (Borradaile & Alford 1987).

Field studies have concentrated on metamorphic rocks that have undergone flattening with principal strains $X \geq Y > 1 > Z$. Our previous experiments attempted to investigate the relationships between magnetic fabrics and experimental flattening. However, many significant geological motions occur in macroscopically-ductile displacement zones, commonly termed shear zones, although not all natural examples necessarily conform precisely to the specialized geometries and kinematics of the model originally discussed by Ramsay & Graham (1970). The purpose of the present study is to examine, under experimental conditions, relationships between magnetic susceptibility anisotropy (i.e. magnetic fabric) and strain in shear zones. Because of the non-destructive nature of the magnetic fabric analysis we were able to remove each specimen from the pressure vessel to measure the magnetic fabric and then resume the test with the same specimen.

Our shear zones do not represent idealized simple shear. Rather they produce a deformation involving a

transpressive kinematic pattern with volume loss and compaction within the shear zone and slight deformation of the bounding wall-rocks. Our tests are restricted to room temperature to prevent temperature-induced effects on the magnetic fabric. Nevertheless, ductility of the specimens without cataclasis of mineral grains has been achieved by using Portland cement as a binding medium.

EXPERIMENTAL PROCEDURE

The approach that we adopted, suggested by Mel Friedman, was to use cylinders of relatively strong rock in which our material of interest was inserted along a slanted cut in the cylinder (Fig. 1). This cylindrical specimen assembly, 19 mm in diameter, is then subjected to axial shortening under some suitable confining pressure in a tri-axial rig. Thus the softer material in the slanted precut is subjected to transpression rather than perfect simple shear. Even in the case of shear zones produced experimentally in a *poly-axial* rig, in solid samples of natural limestone (Kern & Wenk 1983), it was not possible to suppress the component of compaction. Schmid *et al.* (1987) have recently made a thorough study of petrofabrics of calcite rocks in shear zone experiments.

In our study some complications arose because we had to determine the changes in magnetic susceptibility anisotropy (*msa*) of the material in the precut zone. Any changes must be attributable to changes in the intrinsic anisotropy of the shear zone material and not due to a shape-effect of the elliptical slice. To overcome these potential difficulties we took several steps. Firstly, we used a precut slice at 55° to the cylinder axis rather than the usual 35° angle (Friedman & Higgs 1981, Rutter *et al.* 1985). This reduces the ellipticity of the slice of material while the shear stresses along the shear zone walls remain the same. Secondly, for the end-pieces of the cylindrical assembly we used Berea sandstone which is suitably strong and has a low susceptibility, 1.84 (±0.3) × 10^{-5} SI units/unit volume. Thirdly, we synthesized a suitably soft material for the shear zone with a high susceptibility. We produced two materials of 'fine-sand' size trapped between sieve mesh sizes of 0.25 and 0.176 mm. One was a quartz–feldspar–pyroxene sand and the other was a crushed sample of pure calcite.

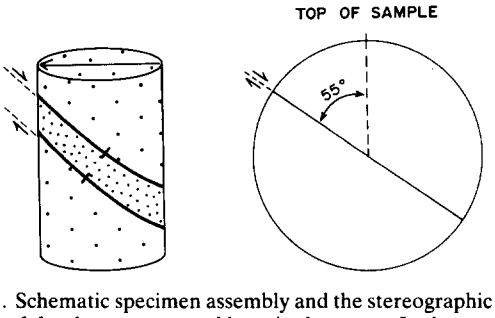

Fig. 1. Schematic specimen assembly and the stereographic representation of the shear zones used later in the paper. In the stereographic view, the plane of this page is termed the *profile plane* of the shear zone.

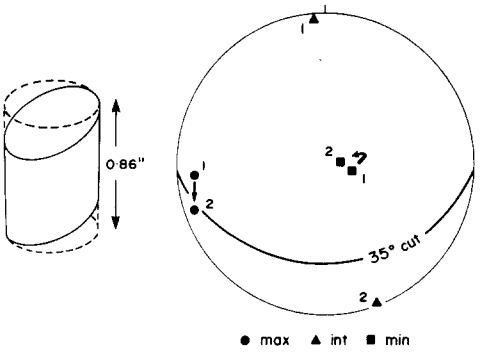

Fig. 2. Changes in anisotropy of magnetic susceptibility of a cylindrical specimen when its ends are ground to a slant.

To each sample was added sieved, crushed and detrital magnetite, of similar grain size, to form about 10% of the bulk weight. The magnetite grains were inequant so that they have the potential for developing an anisotropic magnetic fabric. Each aggregate was then set with 30% dry weight of Portland cement so as to preserve a magnetic fabric with as weak an anisotropy as possible. The cement that we used, when cured, has a low susceptibility of 8.71 (±0.05) × 10^{-5} SI units/unit volume. The cemented aggregates were allowed to cure for at least 28 days before use in order to achieve a uniformly high strength. The bulk susceptibilities of the aggregates had very low anisotropies and high mean susceptibilities of 6.01 (±0.008) × 10^{-2} SI units/unit volume for the quartz–feldspar 'sandstone' and 8.9 (±0.003) × 10^{-2} SI units/unit volume for the calcite aggregate. From the aggregates, drill-cores were made and the slanted discs needed for the shear zones were then sawn and polished so that the discs had plane-parallel sides to within 0.05 mm.

We determined the magnetic susceptibility and its anisotropy by an induction coil instrument provided by Sapphire Instruments of P.O. Box 385, Ruthven, Ontario. To detect any specimen-shape effect on the measurement of susceptibility anisotropy we compared the principal directions of a cylinder of ideal dimensions (i.e. length = 0.82 × diameter) with the thickest possible elliptical disc that could be cut from it (Fig. 2).

Reshaping the cylinder by cutting in this way produced a slight apparent change in the determined principal directions. Further reducing the width of the elliptical slice down to the thickness of about 4 mm, as required for a shear zone test, produced little further change in the apparent positions of the principal susceptibility axes (Fig. 3).

The effects of slice-dimensions on the measurement of the magnitude of anisotropy are very slight. We have used P' (Jelinek 1981) as a measure of the degree of anisotropy (Fig. 4) and we can detect no significant effects of specimen shape in this highly susceptible material.

The specimen assembly for the shear zone tests is shown in Fig. 5(a), in which the elliptical disc of synthetic material is sandwiched between the Berea sandstone end-pieces and inserted in a close-fitting jacket of Teflon.

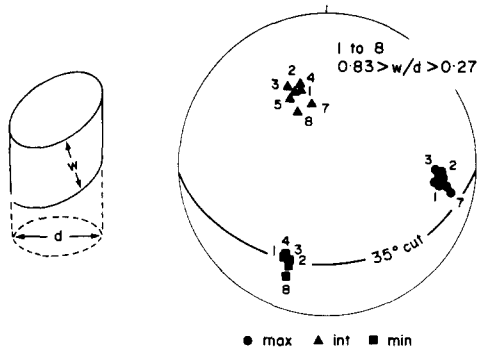

Fig. 3. Changes in magnetic susceptibility anisotropy as a slanted cylinder is reduced in thickness, by grinding, to the slanted disc of the thickness required for the shear zone assembly. Thickness = w, diameter = d.

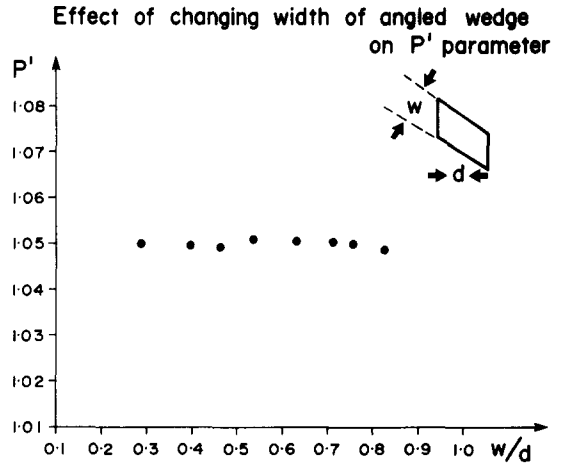

Fig. 4. Changes in the degree of anisotropy (expressed as P' after Jelinek, e.g. see Hrouda 1982) as the slanted cylinder is cut down to a slanted disc in preparation for a shear zone test.

Thus the susceptibility anisotropy of the entire assembly can be measured with no significant contribution from either the jacket or end pieces. This permitted us to deform the same assembly many times and measure the incremental changes in susceptibility anisotropy between successive tests when the specimen assembly was removed from the pressure vessel.

The shear zone fabrics were produced by shortening the specimen assembly in a Donath tri-axial rig. Confining pressure was either 100 or 150 MPa and the permeable specimen assembly was vented to the atmosphere so that the pore pressures are believed to be atmospheric. The shear displacements were produced by advancing the pistons under computer-control at a constant rate of 1.27 (±3%) × 10^{-4} mm s^{-1}. This corresponds to a slip vector of 0.73 × 10^{-4} mm s^{-1} for one shear zone wall relative to the other. This slip is distributed across the shear zones reasonably uniformly at a microscopic scale (see Fig. 5b). The initial shear strain rate is 1.83 × 10^{-5} s^{-1} for a shear zone 4 mm thick, but the rate depends on the initial value of the disc thickness and it increases with the non-linear reduction in disc thickness during the test. In a single test, or 'increment', a shear strain of about 0.025 was usually achieved. The specimen was then removed from the pressure vessel and the magnetic fabric measured before the test was resumed. A sequence of tests on the same sample would eventually achieve a total shear strain between 0.15 and 0.38.

Axial load measurements were made by an internal load cell that requires no frictional corrections and records axial stress with a precision of ±1.0 MPa. Displacements were also electronically recorded with a precision of ±0.01 mm. These measurements are necessary for the on-line computer adjustments of process control in order to achieve constant rates of strain.

MECHANICAL RESPONSE OF THE MATERIALS INVOLVED

The synthetic materials involve a significant proportion of Portland cement and its mechanisms of deformation under the experimental conditions are poorly understood. Cataclasis was the dominant grain-scale deformation mechanism in the quartz–feldspar sand and twinning dominates in the calcite grain-aggregate. However, very significant intergranular motions are evident in all specimens at both 100 and 150 MPa. These are believed to involve grain rotations and sliding in a complex fashion due, at least in part, to the compaction and behaviour of the cement gel matrix. The number of mineral grain contacts increases with advancing strain, compare Figs. 6(a) & (b). Thus it appears that the cement gel collapses and compacts, permitting poorly ordered motions of the grains that we prefer to lump together as 'particulate flow'.

To detect if any special contribution is attributable to the cement matrix we performed stress relaxation tests. Since the geometry and rheology of the specimen assembly is complex we performed the relaxation tests on solid cylindrical specimens. However, we believe that the flow laws may be dependent on strain history and strain geometry so that 'pure shear' and 'simple shear' flow laws may not be equivalent. (G. Borradaile has devised an apparatus to determine flow laws from the discs used in these shear zone tests directly and this work is in progress.)

In the present study stress relaxation has only been performed in axial symmetrical shortening ('pure shear'). This has been done for both synthetic aggregates and for the Berea sandstone used for the wall-rocks. These involve the deformation of a material to some arbitrarily chosen level of strain in steady-state flow, locking the piston in place (relative to the pressure vessel) and then recording the decay of axial stress with time as the elastic energy in the specimen (and the machine) is converted into permanent strain in the specimen. In theory this permits the flow stress to be determined at a wide range of strain rates for the same specimen. It has been pointed out to us by Brian Bayly that stress relaxation analysis *assumes* that the elastic and inelastic responses of the material are simply combined in series and therefore easily separable in analysis. This assumption may or may not be valid depending on

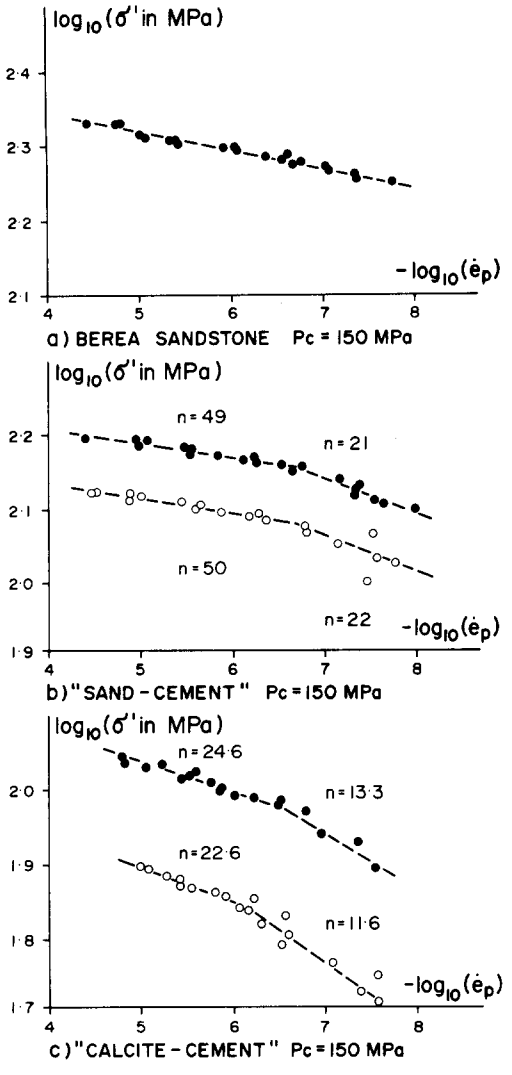

Fig. 7. (a) Stress relaxation results for solid cylindrical specimens of Berea sandstone in 'pure shear'. (Berea sandstone was used for the end-pieces of the specimen assembly.) $\dot{e}_P$ represents the inferred rate of accumulation of permanent strain. This involves a correction for the elastic response of the sandstone, *assuming* that the elastic and inelastic responses are in series, σ' represents the differential stress in MPa. (b) Stress relaxation results for solid cylinders of the quartz–feldspar sand-cement synthetic material in 'pure shear'. n indicates the inverse slope of the linear segments. (c) Stress relaxation results for solid cylinders of the calcite-cement synthetic material in 'pure shear'.

the rheology of the material and warrants further investigation. For the moment, we report the stress relaxation results in the conventional manner inferring the rate of accumulation of permanent strain, $\dot{e}_P$ (e.g. Guiu & Pratt 1964, Rutter & Mainprice 1978). The Berea sandstone shows a gently sloping, linear relationship between flow stress and $\dot{e}_P$ (Fig. 7a). This relationship has been repeatedly found for similar materials at room temperature and low confining pressure (<200 MPa) (Donath & Fruth 1971). This indicates the relative insensitivity of flow stress to strain-rate accompanying cataclasis and particulate flow.

Stress relaxation tests on cylinders of the two synthetic materials show a slightly greater sensitivity of stress to rate of permanent-strain accumulation (Figs. 7b & c). This may be attributed to some contribution of the cement gel. However, the most interesting feature is that all tests show a break in slope at a similar strain rate of approximately $10^{-6.5}$ s^{-1} at various confining pressures (67, 100 and 150 MPa). By contrast with the results for Berea sandstone this encourages us to suggest that there is some significant contribution of the cement gel to deformation mechanisms at the grain-scale. It appears that the response of the cement gel or of the gel interfaces (Neville 1970) with mineral grains shows a modestly greater sensitivity between flow stress and $\dot{e}_P$.

EFFECTS OF SHEAR ON MAGNETIC FABRICS

Twenty-nine different shear zones have been studied at confining pressures of 100 or 150 MPa and the same wall slip-rate of 0.73×10^{-4} mm s^{-1}. Approximately equal numbers of tests were performed on the quartz-rich aggregates and on the calcite aggregates. Most of these tests were interrupted between 4 and 9 times each in order to determine the magnetic susceptibility anisotropy and thereby study the progressive development of the magnetic fabric in a non-destructive manner. Some typical results are reported below.

Silicate aggregates

The effects of shear strain on synthetic quartz–feldspar–pyroxene 'sandstone' have been observed in numerous single step tests, which will not be described here, and in several multiple-step or incremental tests. A typical result (Fig. 8a) shows the tendency for the

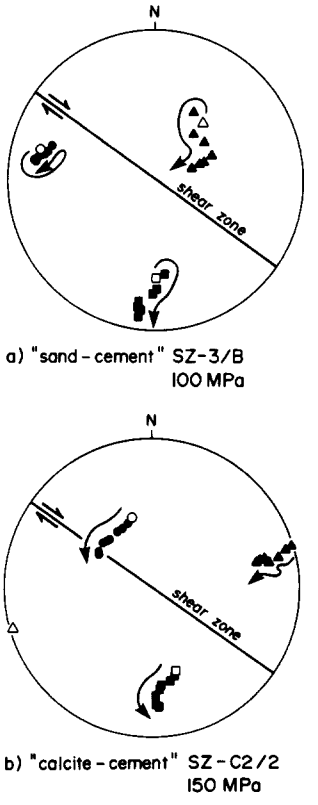

Fig. 8. Progressive change in orientation of magnetic fabric axes (principal susceptibilities) during shear zone formation of the synthetic materials. These equal-area stereograms represent a profile plane of the shear zone.

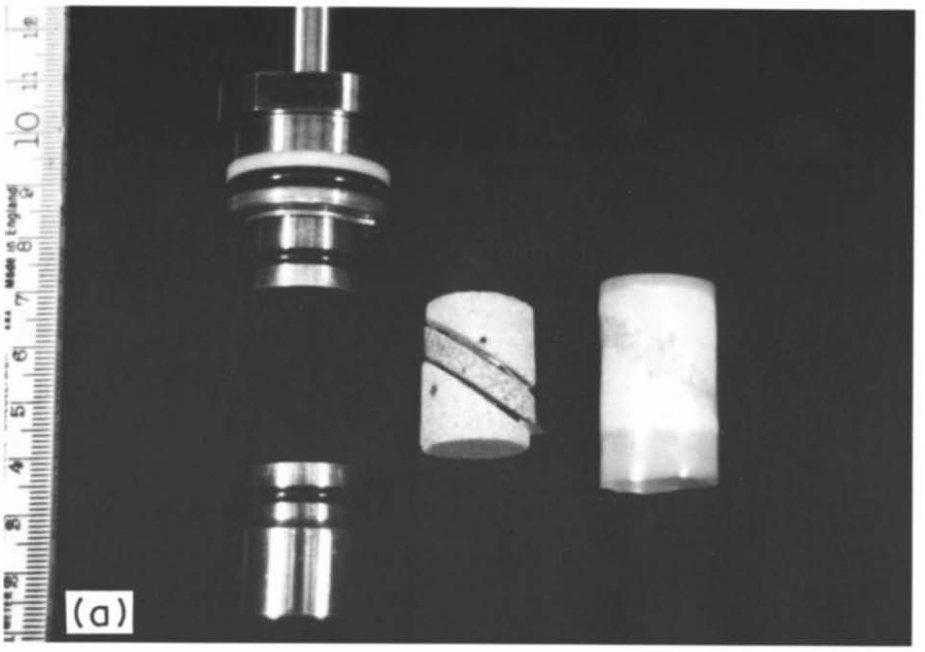

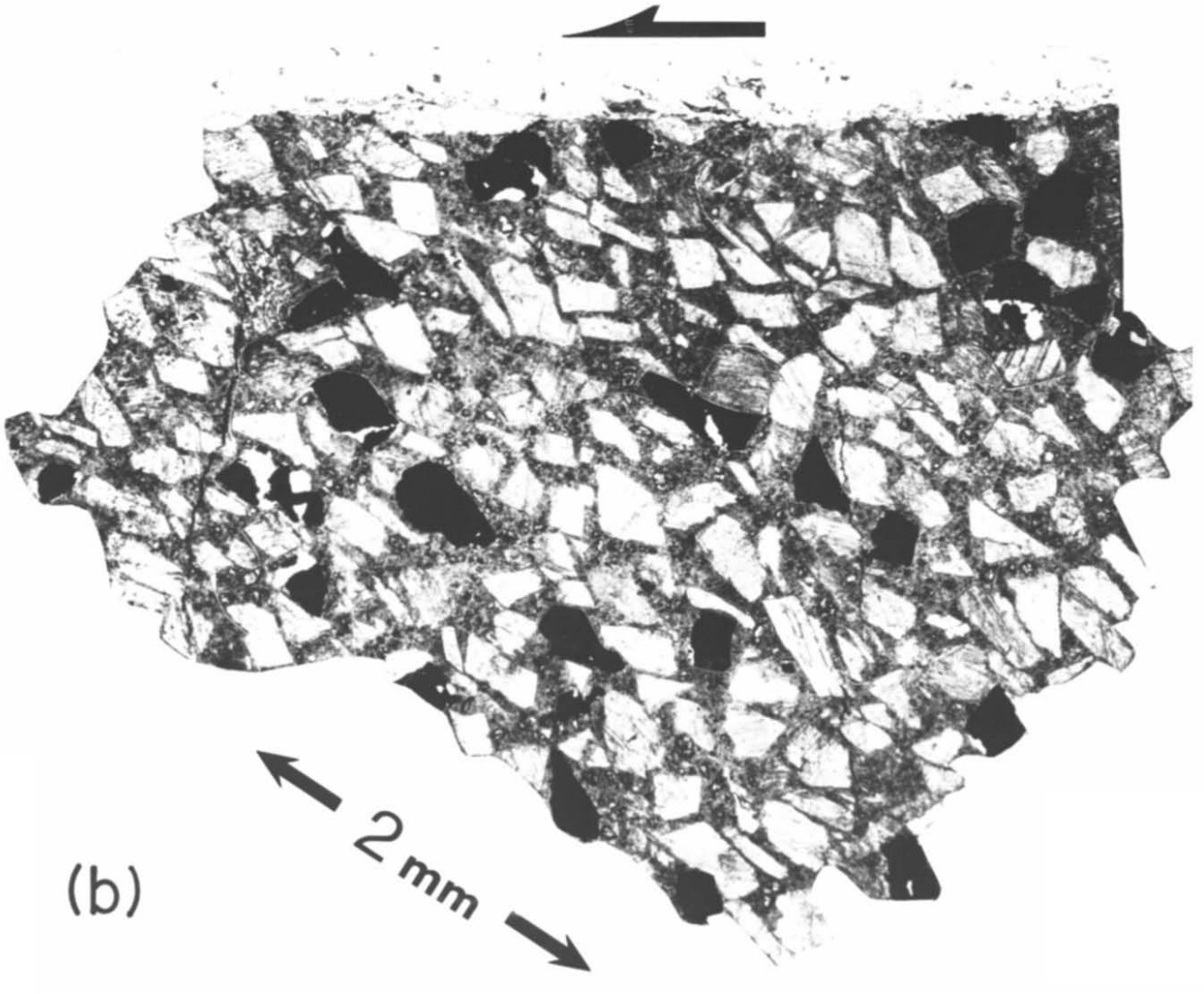

Fig. 5. (a) Photograph of piston and anvil (left), shear zone assembly (centre), and deformed shear zone assembly in its Teflon jacket (right). Note that the anvil is free to slide laterally inside the pressure vessel. (b) Composite microphotograph of a section of an experimental shear zone of a calcite aggregate parallel to the profile plane. Note the preferred orientation of the fabric parallel to the scale bar.

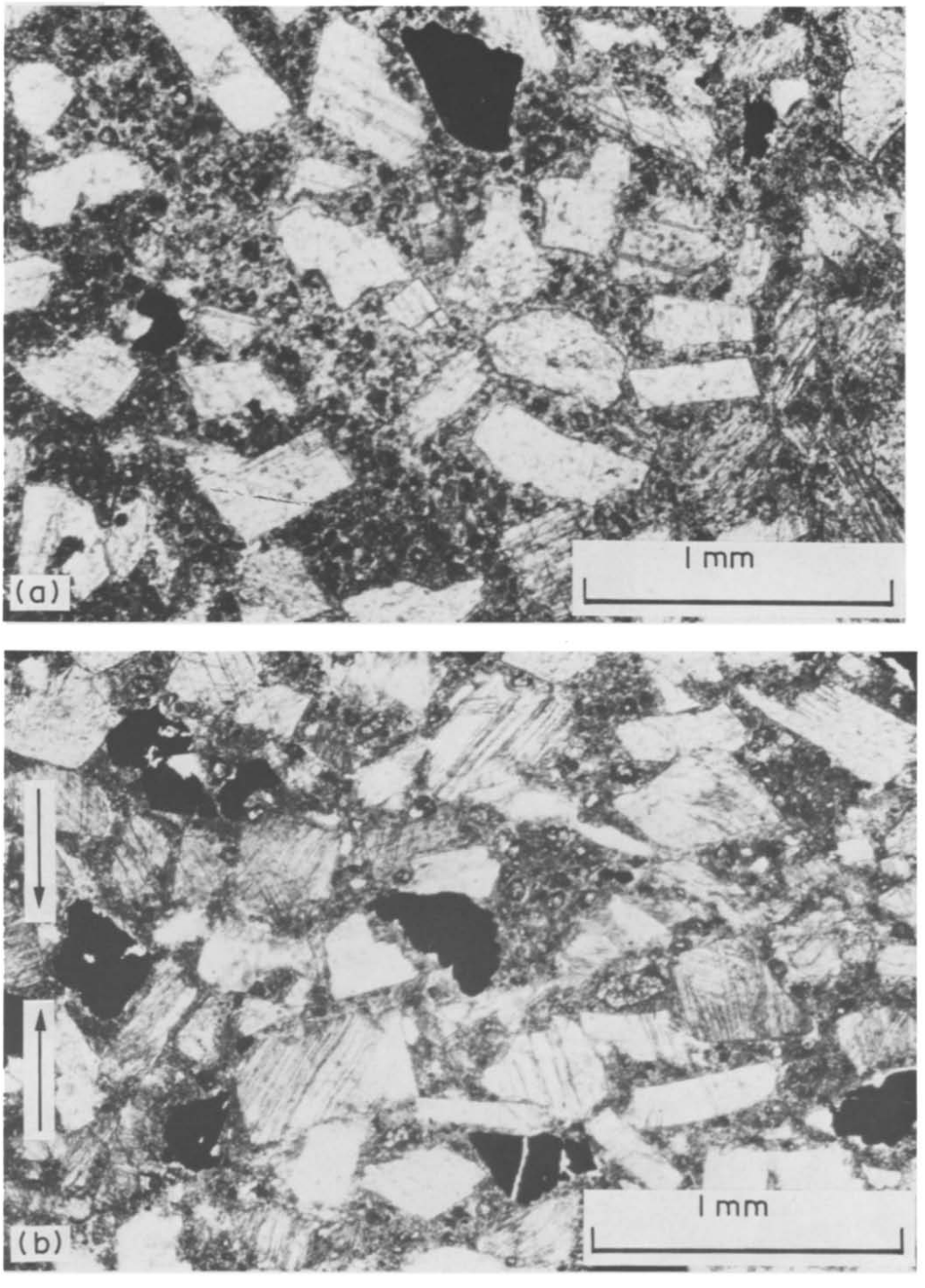

Fig. 6. (a) Pre-deformation texture of calcite–cement–magnetite aggregate. Note spacing of the mineral grains. Height of field of view: 2 mm. (b) Post-deformation texture of the same material after 18% axial symmetrical shortening ('pure shear') at 150 MPa and 10^{-5} s^{-1}.

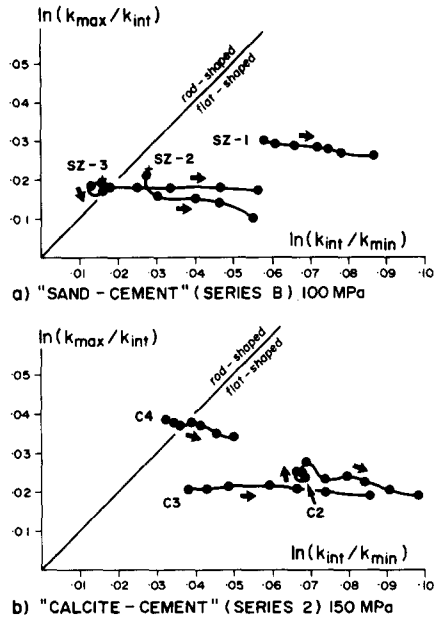

Fig. 9. Logarithmic Flinn diagram for selected shear zone fabrics in progressive deformation. Each line connects points representing the fabric ellipsoid's shape at different stages in the shear zone development. The lines can thus be considered analogous to deformation paths for the magnetic fabric. In all cases the fabric shows progressively greater flattening.

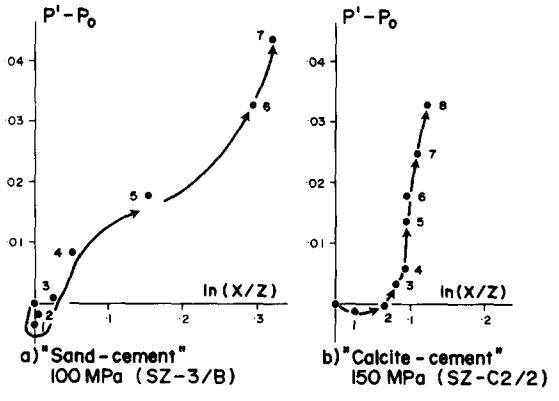

Fig. 10. Relations between the change in degree of anisotropy ($P' - P_0$) and the hypothetical strain ellipse ratio for the shear zone. Such relationships are not universal and only appear where two of the principal susceptibilities initially lie nearly in the profile plane.

minimum susceptibility to migrate into the plane perpendicular to the shear zone and containing the slip vector. (We shall refer to this plane as the profile plane subsequently.) The other two principal directions migrate toward the shear plane if they are not already oriented close to it. We have not been able to detect any tendency for the susceptibilities to align parallel and perpendicular to the schistosity, which is weakly developed in our shear zones even at the maximum shear strain. The shear zones appear quite homogeneous after deformation (Fig. 5b) so we do not attribute the fabrics to combinations of different subfabrics localized by shear along the shear zone walls.

The magnitudes of susceptibility usually describe an ellipsoid of very low eccentricity at the start of the deformation. This is represented by a point near the origin of the Flinn-type deformation plot (Fig. 9). With advancing deformation the successive anisotropy ellipsoids may, in some cases, initially move toward a plane-strain type of shape but as strain progresses they inevitably move further into the field of oblate ellipsoids.

Despite the complex nature of the deformation in these shear zones we have been able to detect an increase in magnetic anisotropy, P', with strain. We do not suggest a significant correlation but the *change* ($P' - P_0'$) in degree of anisotropy of susceptibility does show a fairly steady increase with ln (X/Y), where X/Y are the axes of the hypothetical strain ellipse that would be produced by homogeneous, perfect simple shear in such a zone. The zone is not a perfect case of simple shear so that the strain is slightly underestimated (usually by about 5–10%) because of the component of compaction. The resulting correlations between susceptibility and strain are not considered to have any universal application. They do, however, indicate that any relationship of this nature must take into account the initial magnetic fabric, particularly its orientation, because the relationship illustrated in Fig. 10 involves the *change* in magnetic anisotropy. The initial slow changes, or even early decreases in anisotropy, are due to the initially unfavourable orientations of the bulk fabric ellipsoid with respect to strain-induced change.

Calcite aggregates

In terms of susceptibility orientations the calcite aggregates show similar patterns. The minimum susceptibility direction rotates away from the shear zone (Fig. 8b) or is relatively stable if it is already at a high angle to it. The other two susceptibilities tend to migrate toward the shear zone or toward the orientation of its inclined weak planar grain fabric (Fig. 5b). The rotation is usually more rapid and more complete than for the silicate aggregates at the same strain. The shape of the magnetic fabric ellipsoids usually progresses steadily into the field of flattening (Fig. 9b) as with the silicate aggregates. In contrast, the calcite grains deform so as to produce a slightly constricted fabric. Like Schmid *et al.* (1987) we note that in experimental shear zones the calcite develops twins in only a restricted range of orientations (compare Fig. 5b for shear zone with Fig. 6b for axial-symmetrical shortening).

The intensity of magnetic fabric development is greater in calcite aggregates, presumably because the greater grain-deformation of the calcite permits greater rotation of the interspersed magnetite grains. The change in anisotropy degree ($P' - P_0'$) increases with ln (X/Y) in the shear zones formed by calcite (Fig. 10b); again this is more rapid than for the silicate aggregates at the same strain (Fig. 10a).

The calcite aggregates also have been deformed in conventional triaxial tests where solid cylindrical samples were subjected to incremental axial shortening (Borradaile & Alford 1987). In this way a macroscopically coaxial strain history was imposed on the specimen,

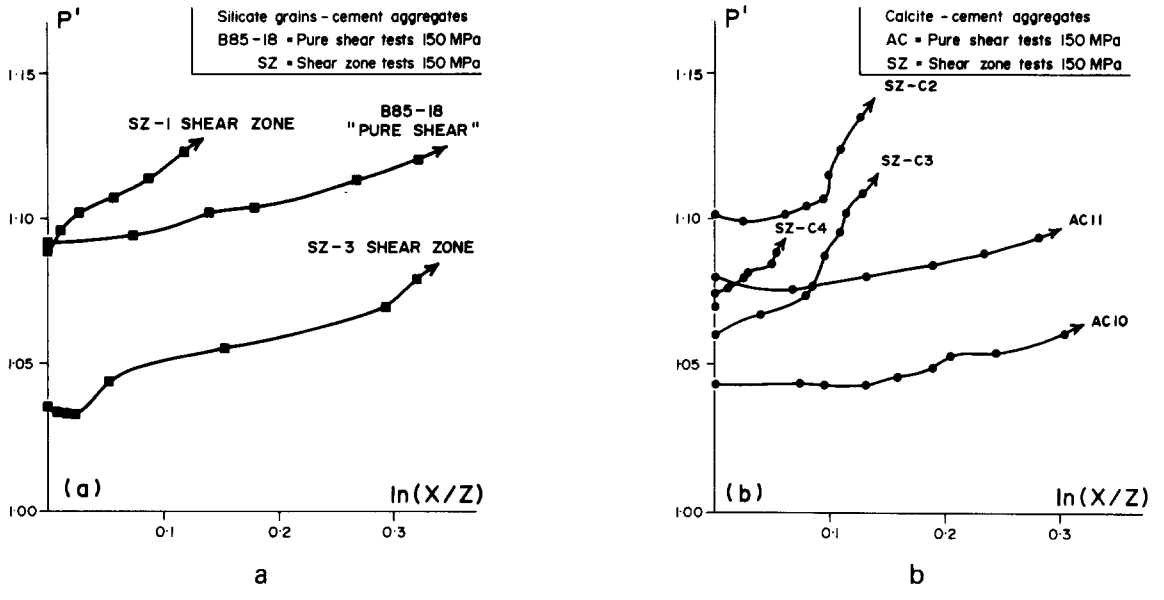

Fig. 11. (a) and (b) The logarithmic strain ellipse ratio X/Z represents the bulk homogeneous strain for the axially shortened specimens and for the shear zones, as appropriate. The degree of magnetic anisotropy, P', increases much more rapidly with advancing strain in the case of the transpressive shear zones for the calcite aggregates.

approximating 'pure flattening' since the specimen is able to expand against the confining pressure oil in all directions perpendicular to the cylinder axis. A comparison has been made (Fig. 11a & b) of the relative efficiencies of the non-coaxial history (the shear zone tests) and the overall coaxial strain history (the pure shear tests). As a basis for comparison the magnetic anisotropy degree, P', has been plotted against the logarithmic bulk strain ratio (ln X/Z) for the pure shear tests. For the shear zone tests P' is plotted against the logarithmic strain ratio for the theoretical strain ellipse that would be produced by homogeneous simple shear with the *same shear strain* as that realized in the (transpressive) shear zone. This slightly underestimates the strain but the measures of strain are broadly comparable for the two types of test. It is found that the non-coaxial, transpressive deformation is much more efficient than coaxial compression in generating a magnetically anisotropic fabric in the calcite aggregates (Fig. 11b). This has not been confirmed, to the same degree, for the silicate aggregates (Fig. 11a). This leads us to suggest that in the case of the calcite aggregates the flow laws may also differ between axial shortening experiments and shear zone experiments.

Hitherto, experimentally determined flow laws have been deduced from axial-symmetrical shortening. Our experiments suggest that these may not be appropriate for extrapolation to natural situations in which non-coaxial strain histories prevail. Nevertheless, Schmid *et al.* (1987) found some indication that the flow laws for 'pure shear' and 'simple shear' were equivalent for marbles when suitable allowance was made for different geometries. These differences could also arise because our synthetic material is oriented in shear zones with a stronger flattening component and is of a constitution which compacts and undergoes transpression.

DISCUSSION AND CONCLUSIONS

The magnetic fabric ellipsoid axes may change in orientation chiefly due to rigid-body rotation of magnetite because little microscopic evidence of deformation of magnetite has been found. However, internal changes in the shape of the magnetic domains cannot be ruled out. The shape of the fabric ellipsoid may therefore have changed primarily in response to the intensity of the preferred *dimensional* orientation of the initially inequant grains of clastic magnetite. Thus the magnetic evidence, whether directional or in terms of susceptibility magnitudes, only reflects the alignment of magnetite. The aggregates deform by compaction of the cement gel, flattening of the zone in the axial direction, shear and, especially in the case of calcite aggregates, by grain deformation (Fig. 5b).

The magnetic fabric ellipsoids developed flatter shapes as a result of the alignment (and possible strain) of magnetite grains. This was more extreme in the calcite aggregates because the greater deformation of calcite grains permitted magnetite to align more easily than in the silicate aggregates. In the latter, the weaker alignment of magnetite was achieved chiefly by intergranular motions of the mineral grains in the compacting cement gel. We may term this intergranular flow (Paterson 1987, p. 37) or particulate flow. It is characterized by grain strain being much less than bulk strain as in these experiments. The shape of the magnetic ellipsoid corresponds broadly to that of the grain shapes that dominate in the deformed aggregate. The grain shapes lie in the flattening field ($X/Y < Y/Z$) although the shear zones have not bulged out of the cylindrical specimen assembly either parallel or perpendicular to the direction of shearing. The compaction of the cement gel, shown by the increase in the number of grain contacts during defor-

mation (cf. Figs. 6a & b), has accommodated the flattening of the grains without lateral spreading of the discs. Lister & Williams (1979) note also that flattened textures can occur in (simple) shear zones as a scale-related phenomenon.

Transpression is much more efficient than axial-symmetrical compression in increasing the anisotropy of the magnetic fabrics. It may be that the simple shear component is so effective because it is a plane strain, whereas axial-symmetric compression imposes a more dispersed movement pattern on the trajectories of spinning grains. Kern & Wenk (1983) have noted a similar effect with regard to the efficiency of developing calcite polycrystal petrofabrics, for which an intrinsic material effect was invoked.

We have not been able to determine whether the magnetic fabric ellipsoid is a useful kinematic indicator of shear sense in these zones. The dimensional fabric of the matrix grains does indicate the fabric asymmetry (Fig. 5b) because those grains are strongly non-equidimensional. However, the magnetic fabric which is controlled by magnetite grains, does not seem capable of defining the preferred orientation (or L–S fabric) to the same degree for several possible reasons. Firstly, the shear zones are transpressive, involving considerable shortening and compaction in the axial direction of the specimen assembly. The component of simple shear starts to develop a weak preferred dimensional orientation early during shear, in perfect simple shear this would be at 45° to the shear zone walls. However, it soon rotates to an orientation in which the component of axial shortening tends to spin the fabric in the opposite sense, counteracting the rotation due to the component of simple shear (Fig. 12). These competing effects may combine to inhibit the development of a suitably oriented magnetic S-fabric and keep it in a stable orientation in our tests. Secondly, the final amounts of shear are quite modest, <0.38 in all cases. This may be too small to develop a substantial obliquity of the magnetic S-fabric.

A further complication that could be of some value to field geologists is that the calcite fabrics are slightly constricted in the shear zones ($L \geqslant S$) whereas the magnetic fabrics are planar ($S > L$). Discrepancies between the shapes of magnetic and petrofabric (or strain) ellipsoids *within the field of flattening* have been reported from natural rocks (e.g. Borradaile & Tarling 1984), but we should now be aware that it is possible to generate greater discrepancies.

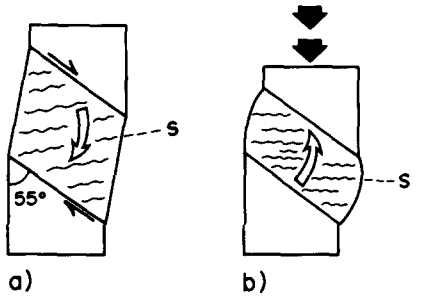

Fig. 12. (a) Simple shear alone would tend to spin the S-fabric counterclockwise in this simplified cartoon of the specimen assembly. (Note that previous assemblies used by other authors have had discs inclined at 35° to the cylinder axis.) (b) Axial compaction combined at a later stage of shearing tends to spin the S-fabric clockwise.

In summary, our results show that the net effect of experimental transpression is to spin the magnetic fabric ellipsoid so that it quickly comes to lie with its minimum susceptibility axis at a high angle to the shear zone walls and the other two axes close to the plane of shear. In some tests the magnetic fabric stabilized in this orientation despite continued non-coaxial strain.

Finally, it should be noted that to achieve specimen homogeneity we chose magnetite to be of the same grain size as the other major mineral grains. This is useful in one sense, for the magnetite grains should give some indication of the rigid-body component of motion affecting any other grains of similar size, and this will be reflected in the magnetic fabric if it develops in response to the rotation of magnetite grains. Despite these advantages, it should be noted that magnetite grains are often smaller than other grains in nature and may lead to different results. Moreover, the magnetic fabric of a rock may be attributable to magnetite only in part, or even entirely due to other minerals. Magnetite is the only common mineral for which the magnetic fabric ellipsoid indicates preferred *dimensional* orientation. In all other common minerals, whether ferrimagnetic, paramagnetic or diamagnetic, the magnetic fabric ellipsoid is influenced by the preferred *crystallographic* orientation of the grains. In those circumstances the magnetic fabric is influenced strongly by metamorphic processes.

Acknowledgements—This research was funded by N.S.E.R.C. grant A6861 and a B.I.L.D. (Ontario) grant to G. Borradaile. Graham Borradaile wishes to thank Brian Bayly, Mel Friedman, Peter Hudleston and Mervyn Paterson and David Sanderson for helpful suggestions. C. Alford was in receipt of an Ontario Graduate Scholarship during this work.

REFERENCES

Borradaile, G. J. & Alford, C. 1987. Relationship between magnetic susceptibility and strain in laboratory experiments. *Tectonophysics* **133**, 121–135.

Borradaile, G. J. & Mothersill, J. S. 1984. Coaxial deformed and magnetic fabrics without simply correlated values of principal magnitudes. *Phys. Earth Planetary Int.* **35**, 294–300.

Borradaile, G. J. & Tarling, D. H. 1981. The influence of deformation mechanisms on the magnetic fabrics of weakly deformed rock. *Tectonophysics* **77**, 151–168.

Borradaile, G. J. & Tarling, D. H. 1984. Strain partitioning and magnetic fabrics in particulate flow. *Can. J. Earth Sci.* **21**, 694–697.

Donath, F. A. & Fruth, L. S. 1971. Dependence of strain-rate effects on deformation mechanism and rock-type. *J. Geol.* **79**, 347–371.

Friedman, M. & Higgs, N. G. 1981. Calcite fabrics in experimental shear zones. In *Mechanical Behaviour of Crustal Rocks* (edited by Carter, N. L. *et al.*). *Am. Geophys. Un. Geophys. Monogr.* **24**, 11–27.

Guiu, F. & Pratt, P. L. 1964. Stress relaxation and the plastic deformation of solids. *Phys. Status Solidii* **6**, 111–120.

Hrouda, F. 1982. Magnetic anisotropy of rocks and its application in geology and geophysics. *Geophys. Surv.* **5**, 37–82.

Jelinek, V. 1981. Characterization of magnetic fabrics of rocks. *Tectonophysics* **79**, 563–567.

Kern, H. & Wenk, H.-R. 1983. Calcite texture development in

experimentally induced ductile shear zones. *Contr. Miner. Petrol.* **83**, 231–236.

Lister, G. S. & Williams, P. F. 1979. Fabric development in shear zones: theoretical controls and observed phenomena. *J. Struct. Geol.* **1**, 283–297.

Neville, A. M. 1970. *Creep of Concrete: Plain, Reinforced and Prestressed*. North-Holland, Amsterdam.

Paterson, M. S. 1987. Problems in the extrapolation of laboratory rheological data. *Tectonophysics* **133**, 33–43.

Ramsay, J. G. & Graham, R. H. 1970. Strain variation in shear belts. *Can. J. Earth Sci.* **7**, 786–813.

Rutter, E. H., Atkinson, B. K. & Mainprice, D. H. 1978. On the use of the stress relaxation method in studies of the mechanical behaviour of geological materials. *Geophys. J. R. astr. Soc.* **55**, 155–170.

Rutter, E. H., Peach, G. J., White, S. H. & Johnson, D. 1985. Experimental "syntectonic" hydration of basalt. *J. Struct. Geol.* **7**, 251–266.

Schmid, S. M., Panozzo, R. & Bauer, S. 1987. Simple shear experiments on calcite rocks: rheology and microfabric. *J. Struct. Geol.* **9**, 747–778.